Study of Modeling and Simulation of Direct Contact Membrane Distillation

Mokhless boukhriss, Habib ben bacha, Kamel Zarzoum and khalifa Zhani

Abstract— Invented in 1960s, membrane distillation is an emerging technology for water treatment attracting more attention since 1980s. There are four configurations of membrane distillation including air gap membrane distillation (AGMD), direct contact membrane distillation (DCMD), sweep gas membrane distillation (SGMD), and vacuum membrane distillation (VMD). DCMD and vacuum enhanced DCMD (VEDCMD), a variant of DCMD, were employed in this research. The objective of this study is to develop design tools for scale up of DCMD by analyzing the characteristics of membrane suitable for DCMD, influences of membrane structure (hollow fiber membrane) and pressure on membrane performance, and modeling the energy efficiency of DCMD with varied process parameters.

Index Terms— direct contact membrane distillation; Modeling; simulation; Heat and mass transfer;

1 INTRODUCTION

THE modeling of the membrane distillation in general relate to the major factor as the supply temperature , temperature of the permeate , the overall mass transfer and heat transfer processes related to the properties of the membranes , namely the porosity , pore size etc. . [1, 2, 3, 4], which are important for the design of membrane, but they are less for the design process. Although a model based on measurable parameters engineering is very important for the extension of MD, there are very few articles in the literature have focused on this subject, and patterns of previous processes reported include only the flow dependency on the duration of the membrane of the hollow fiber membranes [5], but does not include the phenomena of flat sheet membranes. Therefore, the objective of this paper was to develop mathematical models adapted to the design process and verify the model.

2 PRESENTATION OF MD

2.1 Basic principles of MD

MD was a membrane separation process combining with membrane technology and evaporation, and the membrane used was hydrophobic micro-porous membrane which could not be wetted by pending solutions. One side of membrane exposed to warm pending solutions directly (hot procedure side), the other side exposed to cold water solutions directly or indirectly (cold procedure side). Volatile components in hot procedure side evaporated in membrane surface, enter cold procedure side through membrane, and condensed into liquid phrase. Other components block off in hot procedure side by hydrophobic membrane and thus realize the objective of compounds separation and purification. MD was the process that transferred heat and quality simultaneously, and mass transfer impetus was steam differential imposed by components permeating through the both membrane sides.

2.2 Membrane configuration

In this section, different MD configurations that have been utilized to separate aqueous feed solution using a micro-porous hydrophobic membrane will be addressed.

2.2.1 Direct Contact Membrane Distillation (DCMD)

In this configuration (Fig. 2), the hot solution (feed) is in direct contact with the hot membrane side surface. Therefore, evaporation takes place at the feed-membrane surface. The vapor is moved by the pressure difference across the membrane to the permeate side and condenses inside the membrane module. Because of the hydrophobic characteristic, the feed cannot penetrate the membrane (only the gas phase exists inside the membrane pores). DCMD is the simplest MD configuration, and is widely employed in desalination processes and concentration of aqueous solutions in food industries, [7–10] or acids manufacturing [11]. The main drawback of this design is the heat lost by conduction.

- *Mokhless Boukhrissis currently pursuing Ph.D degree program in mechanical engineering in school national engineering of sfax, Tunisia, PH-+21698554615. E-mail: mokhlessiset@yahoo.fr*
- *Habib ben Bacha is professor in mechanical engineering in King Saud UniversityUniversity, Arab Saoudi, PH-+966506678408 E-mail: benbacha@yahoo.fr*
- *Kamel Zarzoum currently pursuing Ph.D degree program in mechanical engineering in school national engineering of sfax, Tunisia, PH-+21654033921 E-mail: kamelissat@hotmail.com*
- *Khalifa Zhani Ph.D degree program in mechanical engineering in school national engineering of sfax, Tunisia, PH-+21622726749E-mail: zhani.khalifa@yahoo.com*

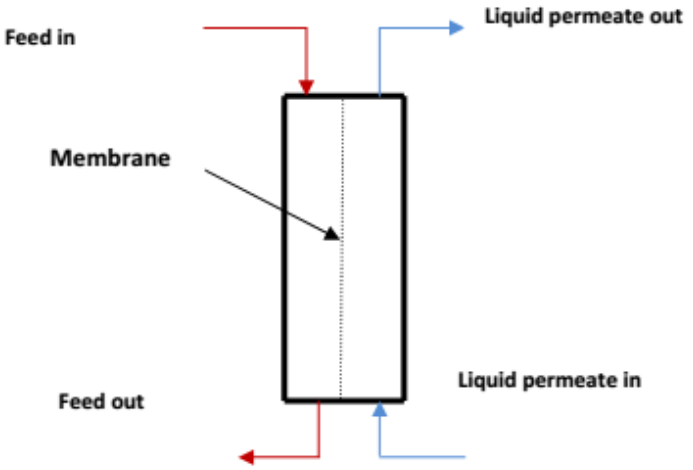

Fig. 1. Direct Contact Membrane Distillation (DCMD)

2.2.2 Air Gap Membrane Distillation (AGMD)

The schematic of the Air Gap Membrane Distillation (AGMD) is shown in Fig. 3. The feed solution is in direct contact with the hot side of the membrane surface only. Stagnant air is introduced between the membrane and the condensation surface. The vapor crosses the air gap to condense over the cold surface inside the membrane cell. The benefit of this design is the reduced heat lost by conduction. However, additional resistance to mass transfer is created, which is considered a disadvantage. This configuration is suitable for desalination [5, 12] and removing volatile compounds from aqueous solutions [9, 13, 14].

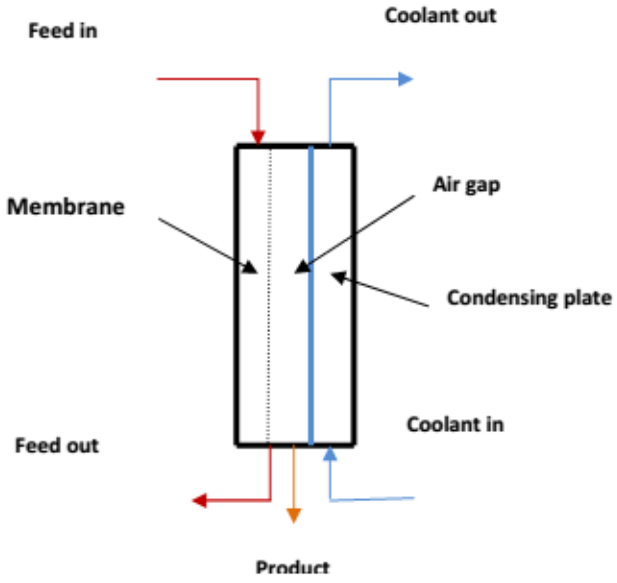

Fig. 2. Air Gap Membrane Distillation (AGMD)

2.2.3 Sweeping Gas Membrane Distillation (SGMD)

In Sweeping Gas Membrane Distillation (SGMD), as the schematic diagram in Fig. 4 shows, inert gas is used to sweep the vapor at the permeate membrane side to condense outside the membrane module. There is a gas barrier, like in AGMD, to reduce the heat loss, but this is not stationary, which enhances the mass transfer coefficient.

This configuration is useful for removing volatile compounds from aqueous solution [12]. The main disadvantage of this configuration is that a small volume of permeate diffuses in a large sweep gas volume, requiring a large condenser. It is worthwhile stating that AGMD and SGMD can be combined in a process called thermostatic sweeping gas membrane distillation (TSGMD). The inert gas in this case is passed through the gap between the membrane and the condensation surface. Part of vapor is condensed over the condensation surface (AGMD) and the remainder is condensed outside the membrane cell by external condenser (SGMD). [15, 16].

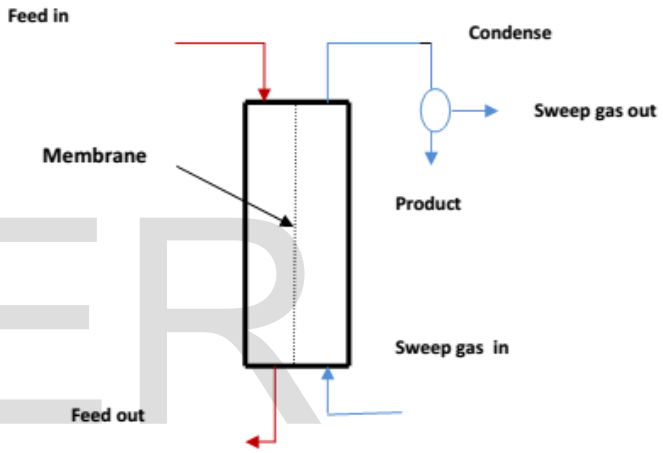

Fig.3.Sweeping Gas Membrane Distillation (SGMD)

2.2.4 Vacuum Membrane Distillation (VMD)

The schematic diagram of this module is shown in Fig. 5. In VMD configuration, a pump is used to create a vacuum in the permeate membrane side. Condensation takes place outside the membrane module. The heat lost by conduction is negligible, which is considered a great advantage [6]. This type of MD is used to separate aqueous volatile solutions [17–18].

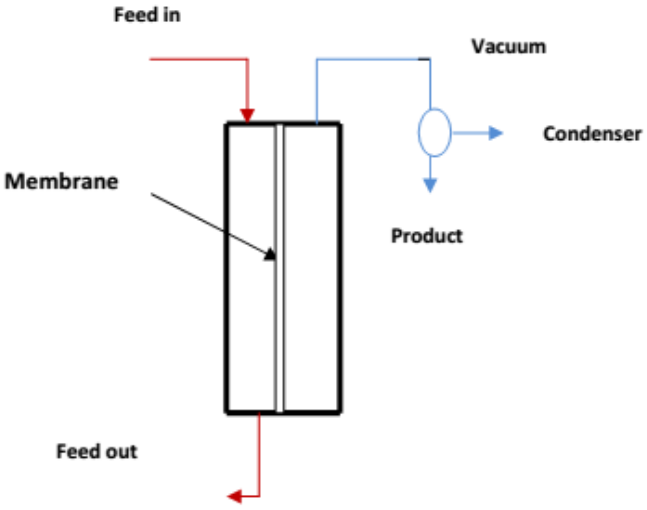

Fig.4. Vacuum Membrane Distillation (VMD)

3 Membrane modules

3.1 Plate and frame

The membrane and the spacers are layered together between two plates (e.g. flat sheet). The flat sheet membrane configuration is widely used on laboratory scale, because it is easy to clean and replace. However, the packing density, which is the ratio of membrane area to the packing volume, is low and a membrane support is required. Table n°1 presents some characteristics for flat sheet membranes that were used by some researchers. As can be seen in Table 1, the membrane is used widely in MD applications, such as desalination and water treatment.

Reference	MD processus	Membrane type	Thickness (µm)	Pore size (µm)	Feed solution
[24]	DCMD	TF200	178	0.2	Pure water and humic acid
		PVDF	125	0.22	
[25]	DCMD	PVDF	125	-	Humic acid/NaCl
[26]	DCMD	PVDF	126	0.22	Pure water, NaCl, brackish and seawater
[27]	DCMD	PVDF	-	0.45	Apple juice
[28]	DCMD	PTFE	60	0.1	Pure water
		PTFE	60	0.3	
		PVDE	100	0.2	
[29]	DCMD	PVDF	-	0.4	Pure water, NaCl and sugar
[30]	DCMD	PTFE	55	0.198	Olive mill wastewaters
[10]	DCMD	PVDF	140	0.11	Orange juice
[31]	DCMD	PVDF	120	0.22	Pure water, NaCl
			125	0.2	
[32]	DCMD	PVDF	125	0.22	Pure water and humic acid
[33]	DCMD	Not mentioned	120	0.25	Heavy metals waste
[34]	DCMD	PTFE	55	0.8	Pure water, NaCl, bovine plasma and bovine blood
			90		

Table 1: Presents some characteristics for the membranes that were used by some researchers

3.2 Hollow fiber

The hollow fiber module, which has been used in MD, has thousands of hollow fibers bundled and sealed inside a shell tube. The feed solution flows through the hollow fiber and the permeate is collected on the outside of the membrane fiber (inside-outside), or the feed solution flows from outside the hollow fibers and the permeate is collected inside the hollow fiber (outside-inside) [8]. For instance, Lagana et al. [19] and Fujii et al. [20] implemented a hollow fiber module (DCMD configuration) to concentrate apple juice and alcohol respectively. Also, saline wastewater was treated successfully in a capillary polypropylene membrane [21]. The main advantages of the hollow fiber module are very high packing density and low energy consumption. On the other hand, it has high tendency to fouling and is difficult to clean and maintain. It is worth mentioning that, if feed solution penetrates the membrane pores in shell and tube modules, the whole module should be changed. [8, 22].

3.3 Tubular membrane

In this sort of modules, the membrane is tube-shaped and inserted between two cylindrical chambers (hot and cold fluid chambers). In the commercial field, the tubular module is more attractive, because it has low tendency to fouling, easy to clean and has a high effective area. However, the packing density of this module is low and it has a high operating cost. Tubular membranes are also utilized in MD. Tubular ceramic membranes were employed in three MD configurations:
DCMD, AGMD and VMD to treat NaCl aqueous solution, where salt rejection was more than 99% [23].

3.4 Spiral wound membrane

In this type, flat sheet membrane and spacers are enveloped and rolled around a perforated central collection tube. The feed moves across the membrane surface in an axial direction, while the permeate flows radially to the centre and exits through the collection tube. The spiral wound membrane has good packing density, average tendency to fouling and acceptable energy consumption.
It is worth stating that there are two possibilities for flow in a microfiltration system; cross flow and dead-end flow. For cross flow, which is used in MD, the feed solution is pumped tangentially to the membrane. The permeate passes through the membrane, while the feed is recirculated. However, all the feed passes through the membrane in the dead-end type [22].

4 Mechanism

The mechanism application of the figure.5 for the mass flux (J) in this case is assumed to be proportional to the vapor pressure difference across the membrane, and is given by:

$$J = Cm.(P_2 - P_3) \quad (4.1)$$

Where Cm is the membrane coefficient, Pf and Pp are the vapor pressure at the membrane feed and permeat surfaces, which can found

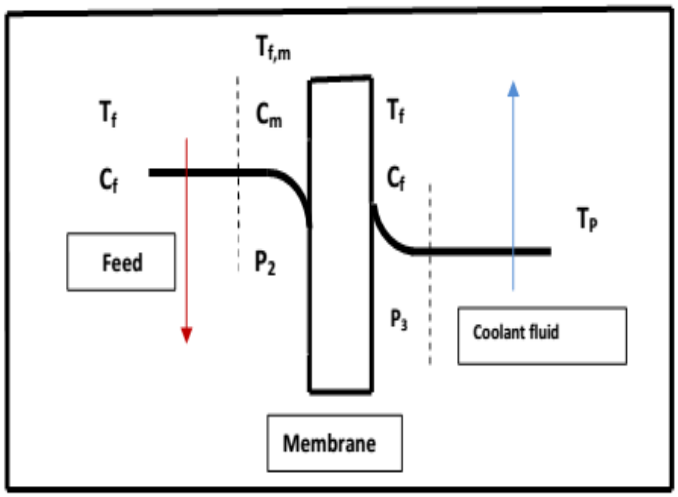

Figure.5 The mechanism application of DCMD

4.1 Membrane permeation flux

Membrane distillation has higher rejection rate but relatively lower flux, and flux affecting factors were outlined as follows [35]:

(1)Temperature: temperature was the main factor affecting permeation flux. For DCMD, enhancing the temperature of solutions in hot procedure side or temperature difference between two sides could result in significant increment of water flux, but not in a linear relationship.

(2) Vapor pressure deficit: permeation flux increased with the increasing of vapor pressure deficit between both membrane sides, and a linear relationship was obtained.

(3) Feed concentration: with the increasing of feed concentration, flux of nonvolatile solute water solutions decreased, while that of volatile increased.

(4) Feed flow rate: Increasing feed flow or cooling water flow could result in flux increment.

(5) Distillation time: due to the process of distillation, membrane pore infiltration resulted in the reflux from the permeation side stream to feed, and membrane pollution caused the reduction of flux. Therefore, with the increasing of distillation time, flux reduction occurred.

(6) Membrane material and structure: hydrophobic microporous membrane was used in MD, and structure parameters affecting water flux were mainly as follows: pore size, porosity and membrane thickness.

5. Theoretical model for direct contact membrane distillation (DCMD)

In the direct contact membrane distillation, mass transfer (evaporation) is coupled with the heat transfer. Therefore, a complex relationship between the mass and heat transferred through the membrane has to be solved to predict the flow from the feed inlet temperature or membranes of different sizes, it was found that the coefficient of calculating total mass transfer is not substantially varied when the hydrodynamic conditions (conditions of turbulence or boundary layer) were constant, but differ greatly speeds the flow (Fig. 6). Based on this finding, a simple model was developed to predict flux from different temperatures and heights membrane using the overall mass transfer coefficient experimentally obtained mass at the same velocity, instead of calculating a transfer coefficient local ground. This model provides a simple tool to estimate the flow of a large sheet of membrane based on the results from the test results of small modules, and can provide an approximate reference point for the design of a driver module and process. From this model, the temperature profile along the membrane at a given flow rate may also be described. Furthermore, it can be used as a technique to compare the performance of the membranes.

For a given after figure .6 of DCMD above system, it can be expected that the flux (J) depends on many parameters and a general relation can be written

$$J = f(A, Tf, Tp, \dot{m}_p, \dot{m}_f, C_{membrane}, U)$$

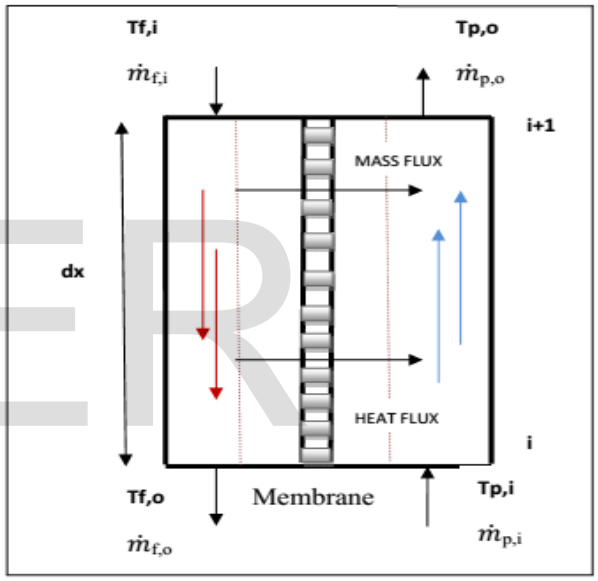

Figure .6: of DCMD above system

Here, $\dot{m}_p$ and $\dot{m}_f$ are the mass flow rates for the cold side and the hot side. In addition, the following assumptions have been made to further simplify the model:

1. no heat loss through the wall of the module into the atmosphere , which is supported by a calculated heat loss through the wall of less than 3 W , which is less than 1 % of the heat loss from the load , and no difference in flow or energy efficiency experiments with and without thermal insulation
2. Specific heat of evaporation and condensation does not change with the concentration on the basis of the results RG Lunnon [22],
3. With a given speed at a given, both U and Cglobal membrane are constant,
4. There is no temperature gradient across the membrane perpendicular to the flow direction (i.e. the direction of the width of the module),
5. Balance mass transfer, the mass of permeate through the membrane can be neglected, based on the experimental

finding that the maximum recovery from a single pass is 1.1 % - 4 % in this study,

6. balance the heat transfer, sensible heat carried by the permeate can be neglected because it is usually less than 3% of the total sensible heat energy carried by the steam transferred to the cold side . For example, the temperature difference between the hot interface and the cold mass flow is approximately 14 ° C, so that the temperature increase due to the sensible heat on the cold side is less than 0, 17 to 0.3 ° C (based on 1.1 - 2 % maximum single recovery), which is about 1.7 - 3 % of the total heat transferred from the steam and heat conduction.

Under these assumptions and equations for different models of mass transfer (4.1) can be simplified all [36], the flux can be expressed as follows:

$$J = G_{loat}.(P_{rf} - P_{rp}) \qquad \text{Eq. (5.1)}$$

Cglobal includes phenomena where mass transfer in the boundary layer and membrane.

Figure 4.1 shows the heat transfer element and a mass in a module DCMD flat sheet. In this element, the variation of the thermal energy from the hot side may be described as follows:

$C_{p,f}\ m_f .(T_{f,i+1} - T_i) = -(J_{Hlatent}.dA + U(TF - Tp).dA)$ Eq. (5.2)

Where Tf, Tf and i +1 , i are the temperatures and ith and (i +1) th are the points, and Cp,f is the specific heat of the food.

For, where W is the width of the membrane, the relationship between the temperature change and the displacement flow can be expressed as,

$$dTf = -\frac{w(JiHlatent + U(Tf,i - Tp,i)}{Cp,frhf}.dx \qquad \text{Eq. (5.3)}$$

Accordingly, the temperature change of the power supply after the current passes each element can be written as follows:

$$\Delta Tf,i = -\frac{Cglobal\left[EXP - EXP\left(23.1964 - \frac{3814.44}{TP,i+227.02}\right)\right]Hlatent + U(Tf,i - Tp,i)}{Cp,frhf} \qquad (5.4)$$

For this Cglobal and U are assumed to be constant, the temperature of the feed stream (i +1)th may be calculated by:

$$Tf,i+1 = Tf,i - \Delta Tf,i \qquad \text{Eq. (5.5)}$$

Similarly, the temperature of the permeate can be calculated:

$$Tp,i+1 = Tp,i - \frac{mf}{mp}\Delta Tf,i \qquad \text{Eq. (5.6)}$$

Thus, the flow through (i +1) th may be calculated as :

$$Ji+1 = Cglobal(Prf,i+1 - Prp,i+1) \qquad \text{Eq. (5.7)}$$

From which the total flux of the membrane can be calculated as:

$$J = \frac{\sum_{i=0}^{N} JiW\Delta x}{A} - \frac{\sum_{i=0}^{N} Ji\Delta x}{L} \qquad \text{Eq. (5.8)}$$

The above equations can be solved numerically. For streams, an iteration process is required and this process is illustrated in the following algorithm for simulation of DCMD figure.7

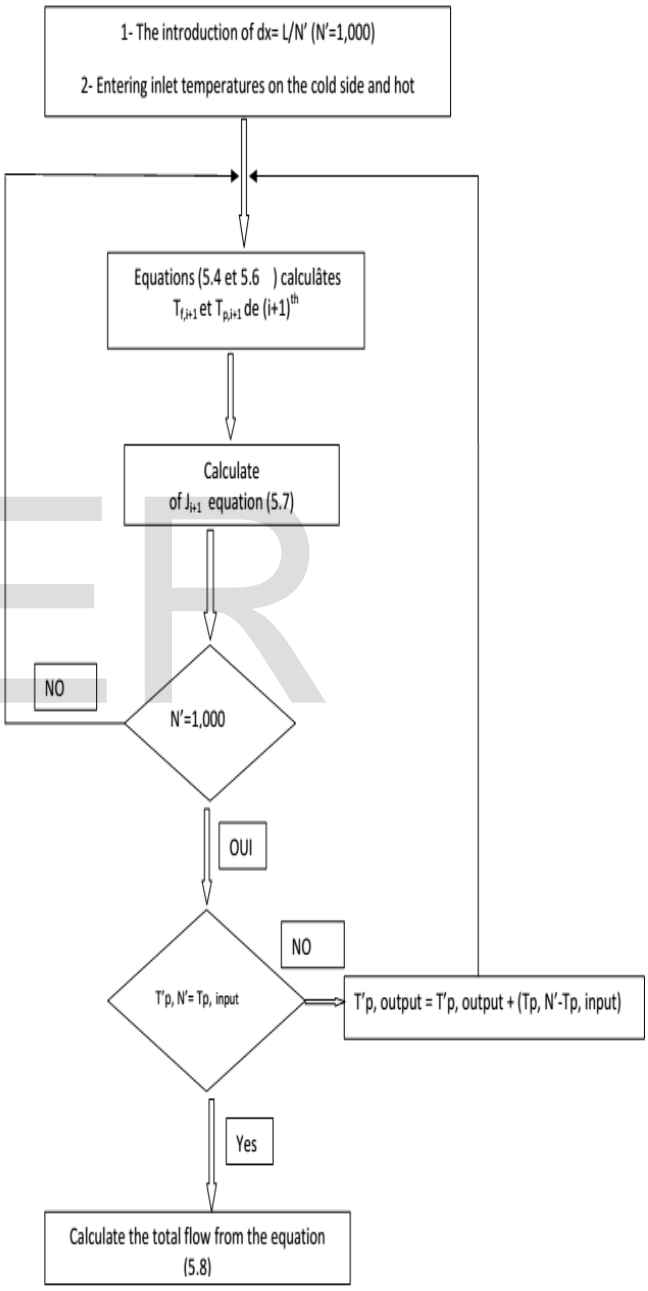

Fig. 7.Algorithm for simulation of DCMD

6. The modeling results

6.1. Validation means of mass transfer coefficients and heat flux prediction

The phenomenon of mass transfer across the membrane that

does not change the properties of membrane, the boundary layer is affected dramatically by the turbulence promoter (spacer) and flow velocities. Consequently, the overall average mass transfer coefficient will also be affected, if the various membranes, spacers and flow velocities are used. In DCMD, variations in the length of the membrane and the temperature have a minor influence on the boundary layer conditions. Therefore, if all the factors that affect the boundary conditions are preset, the calculated total mass, and the heat transfer coefficients in equations (5.2) and (5.3) can theoretically be used to predict the flux in this condition predefined.

The figure. 8. a shows the predicted results that were obtained from a PTFE membrane with a pore size of 1 micron, the coefficients of mass transfer and heat medium flow was calculated for each model that is used. Thus, the weight coefficients and average overall heat transfer is acceptable for predicting the flow at a given rate.

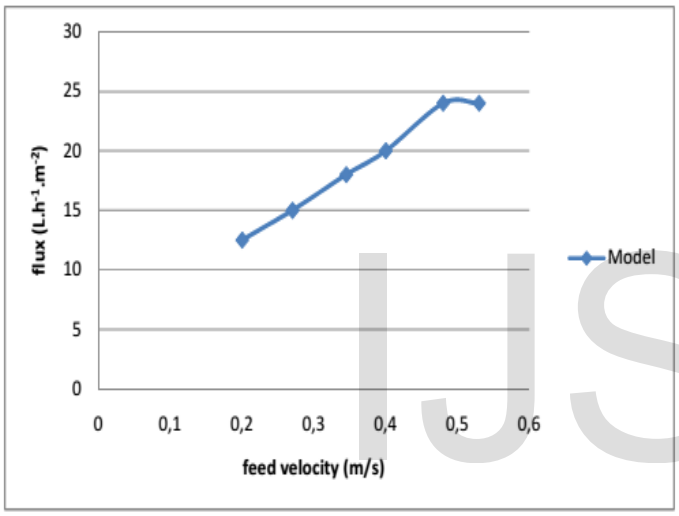

Fig.8.a: modeling results at different speeds to the flow regime

In the model, the local flow of each element was calculated from the weight and average heat transfer coefficient on the basis of equations of the assembly of fig. 8.b, and the total flow modeling was calculated by summing the flows of all the elements. However, due to the variation of the temperature profiles in the membrane, the transfer coefficient of the actual local mass (based on the average pore temperature) and the heat transfer coefficient (depending on the viscosity of the fluid) are different in each element. Therefore, it is necessary to confirm if the mean value of the overall mass transfer coefficients and heat is used.

Therefore, it is reasonable to agree that the model coefficients and mass transfer means transfer heat from a temperature used in this model to predict the flow at different temperatures for a given speed (i.e. the similar hydrodynamic conditions). However, variations in flow occur different turbulence regimes and are expected to significantly alter the coefficients of mass and heat transfer global averages.

From which the average overall mass and heat transfer coefficients may be selected or calculated from the curve to the data for predicting the flow at different temperatures in a particular case as shown in fig. 8. B

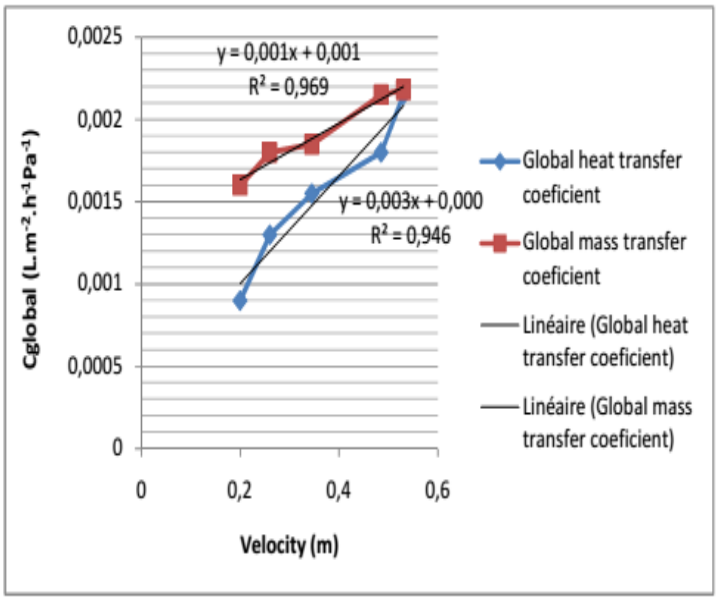

Fig.8. b: Equations coefficients overall average mass transfer and heat for modeling

Fig. 8 Validation of the global averages of coefficients of mass transfer and heat

6. 2. Verification of the model at different temperatures

To verify the model, the transfer coefficient and overall average heat transfer coefficients from mass shown in Fig. 1 it has been used to predict the flux at different temperatures. In the FIG. 9, the results of flows using a DCMD are displayed. The coefficients of heat transfer and overall mass used in the model have been calculated from the experiment food inlet temperature of 60 ° C at 0.4 m / s.

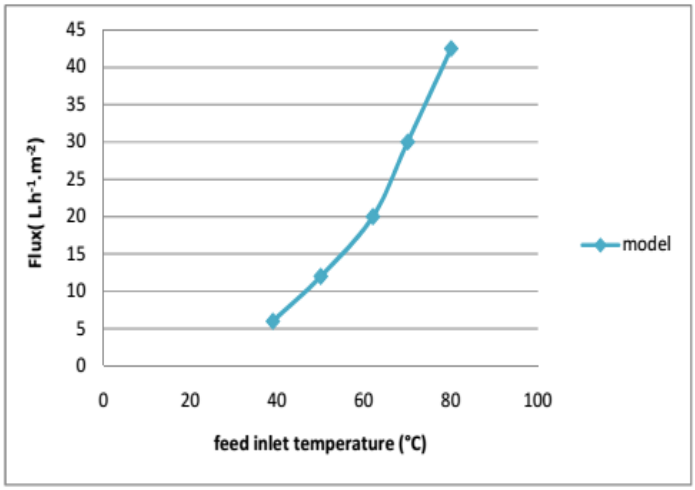

Fig. 9: The modeling results at different temperatures

DCMD

6.3. Verification of the model with different lengths of membrane

The average mass and heat transfer coefficients used in the model were the same for predicting the flow and cooperation to this flow, which are the mean values of all experiments at speeds indicated.

FIG. 10 present modeling results for both this flow. Therefore, the length of the membrane affects the flow of the membrane inlet temperature and given speeds this flow because the short membrane lead to a higher average temperature difference across the membrane because of the reduced residence time heat and mass transfer. Accordingly, it is not appropriate to evaluate the performance of membranes by MD flow, even under conditions of inlet temperature and the same speed, if not including the size of the membrane.

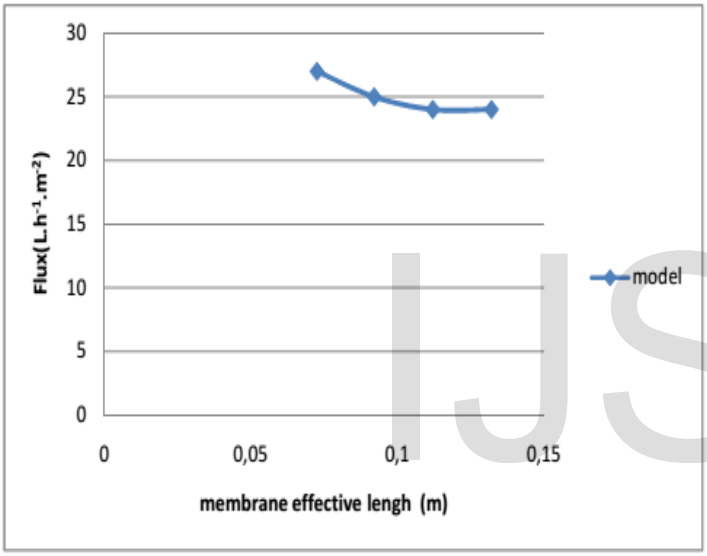

Fig.10: modeling results for different lengths of membrane in the membrane configuration of DCMD 0.5 microns

6.4. The results of mathematical modeling of temperature profile in direct contact membrane distillation

From the model with different membranes, this provides some confidence that the temperature profiles and flow predicted by the model will be accurate at a given speed, and modeling results are based on the overall heat and coefficients mass transfer in FIG. 8.b.

6.4.1. Prediction temperature profile DCMD

Fig 11 shows the prediction of the temperature profile in the two diaphragm chambers. While this flow of temperature profiles on both sides parallel to each other when their speeds are the same.

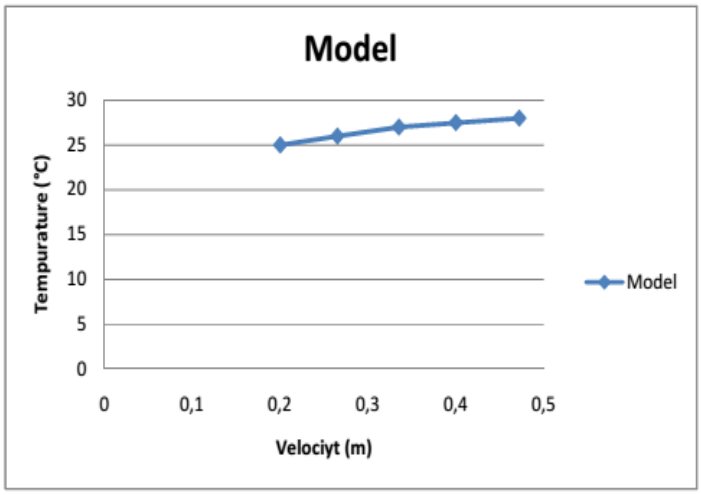

Fig. 11: the temperature profile along the membrane flow DCMD (Feed rate = 0.40 m / s, temperature of cold inlet = 20 ° C, the temperature input power = 60 ° C)

6.1.4.2. Prediction of temperature difference at different speeds

The figure. 12. Shows the average temperature difference across the membrane provided at different speeds using transfer coefficients of heat and mass calculated from the integrated database. From this figure, it was found that the temperature difference increases as the flow velocity becomes higher. Therefore, increasing the flux is proportional to the increase in flow as the latter allow an increase in the mass transfer coefficient with a total temperature difference.

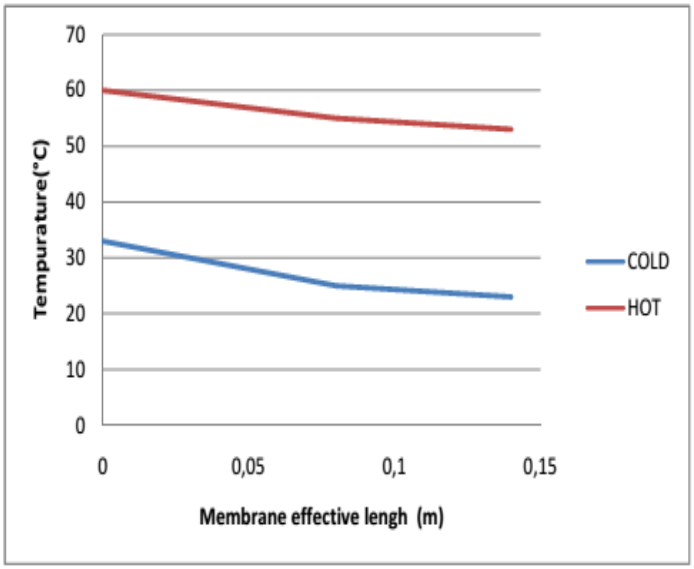

Fig. 12: mean temperature difference across the membranes at different speeds (length of the membrane = 0,145 m, the cold inlet temperature = 20

° C the feed inlet temperature = 60 ° C)

The figure.13. this'd the mean temperature difference across the membranes at different speeds (length of the membrane = 0,145 m, the entrance of cold temperature = 20 ° C the feed inlet temperature = 60 ° C).

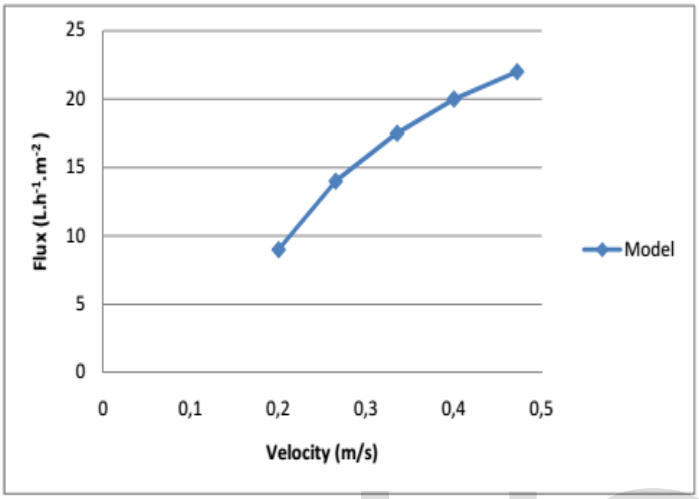

Fig. 13: Cash at different speeds (length = 0.145 m membrane, the feed inlet temperature = 60 ° C, cold inlet = 20 ° C)

This may be caused by different temperature distributions along the flow of the membrane in the DCMD. The stream having the largest temperature difference may be a difference in vapor pressure of less. For example, during water at 10 ° C temperature difference respectively at 45 ° C and 35 ° C a vapor pressure difference of 4000 Pa, and streams from 5 ° C to 60 ° difference respectively C and 55 ° C have a difference in vapor pressure of 4200 Pa.

6. 4.3. Prediction changes flow against of DCMD at different speeds for the power supply

The figure. 14 watches flow changes along the length of the membrane at different velocities. The difference in total flow of from 4.6 to 2.3 reduced L.h $^{-1}$.m $^{-2}$ and 4.7 to 2.3 L.h $^{-1}$.m $^{-2}$, respectively that the flow of DCMD , as the speed increased by a increase of about 0.065 m / s . A similar trend of permeate flux increasingly feed rates has been reported previously [34, 131], and this provides additional support for the reliability of model predictions. Furthermore, the figure also shows that the difference in flow becomes less different speeds more membranes are used.

Therefore, the feed rate will affect the main flow less than the membranes are employed.

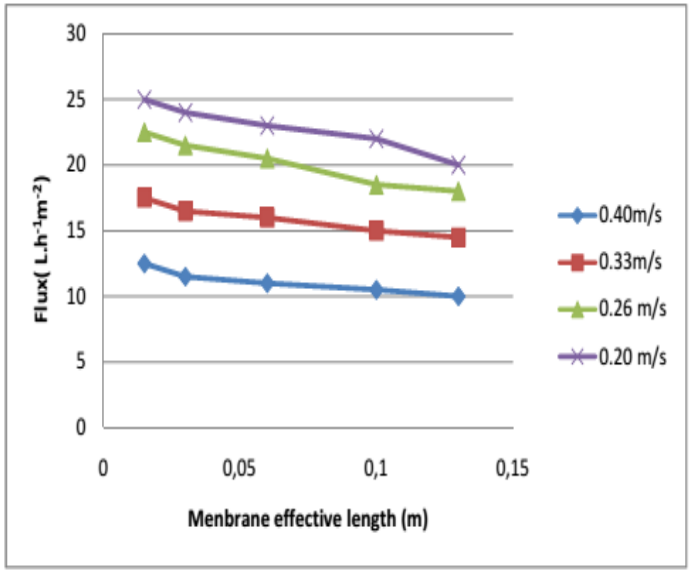

Fig. 14: Changes in flow against the current DCMD in flow direction at different speeds (RSS inlet temperature = 60 ° C, cold inlet = 20 ° C)

Notation

Cmembrane	mass transfer coefficient
Cglobal	global mass transfer coefficient
U	global heat transfer coefficient
H	water protrusion height
Hlatent	latent heat of water vaporization
J	vapor flux
Tp, Tf	permeate and feed bulk temperatures
Tfi, Tfo	feed inlet and outlet temperatures
T1, T2	feed and permeate temperatures at liquid-vapor interface
$\dot{m}_p$, $\dot{m}_f$	are the mass flow rates for the cold side and the hot side

7 Conclusion

In this paper, a mathematical model applied to a direct contact membrane distillation module has been developed. The model is applicable to multicomponent mixtures. A numerical solution procedure based on applied to solve these unknown parameters was presented and it was shown how the analytical

sensitivities can be obtained in a convenient format. The model acts as a black box that calculates the output of the membrane unit and derivative data entry. This formulation supports the implementation of the membrane module in a process simulator. A tool has been obtained which allows the optimization and simulation calculations for hybrid processes involving a membrane distillation unit to direct contact.

REFERENCES

[1] A. S. Josson, R. Wimmerstedt, A. C. Harrysson, Membrane distillation - a theoretical study of evaporation through microporous membranes, Desalination. 56(1985) 237-249.

[2] J. Phattaranawik, R. Jiraratananon, A. G. Fane, Heat transport and membrane distillation coefficients in direct contact membrane distillation, Journal of Membrane Science. 212(2003) 177 -193.

[3] J. Phattaranawik, R. Jiraratananon, A. G. Fane, Effect of pore size distribution and air flux on mass transport in direct contact membrane distillation, Journal of Membrane Science. 215(2003) 75 -85.

[4] F. Lagana, G. Barbieri, E. Drioli, Direct contact membrane distillation: modelling and concentration experiments, Journal of Membrane Science. 166(2000) 1-11.

[5] S. P. Agashichev, D. V. Falalejev, Modeling temperature polarization phenomena for longitudinal shell-side flow in membrane distillation process, Desalination. 108(1997) 99-103.

[6] K.W. Lawson, D.R. Lloyd, Membrane distillation, J. Membr. Sci. 124 (1) (1997)1–25.

[7] V.D. Alves, I.M. Coelhoso, Orange juice concentration by osmotic evaporation and membrane distillation: a comparative study, J. Food Eng. 74 (1) (2006) 125–133.

[8] E. Curcio, E. Drioli, Membrane distillation and related operations — a review,Sep. Purif. Rev. 34 (1) (2005) 35–86.

[9] M.C. García-Payo, M.A. Izquierdo-Gil, C. Fernández-Pineda, Air gap membrane distillation of aqueous alcohol solutions, J. Membr. Sci. 169 (1) (2000) 61–80.

[10] V. Calabro, B.L. Jiao, E. Drioli, Theoretical and experimental study on membrane distillation in the concentration of orange juice, Ind. Eng. Chem. Res. 33 (7)(1994) 1803–1808.

[11] M. Tomaszewska, M. Gryta, A.W. Morawski, Study on the concentration of acids by membrane distillation, J. Membr. Sci. 102 (1995) 113–122.

[12] J. Walton, et al., Solar and waste heat desalination by membrane distillation, College of Engineering University of Texas, El Paso, 2004.

[13] S. Kimura, S.-I. Nakao, S.-I. Shimatani, Transport phenomena in membrane distillation, J. Membr. Sci. 33 (3) (1987) 285–298.

[14] F.A. Banat, J. Simandl, Membrane distillation for dilute ethanol: separation from aqueous streams, J. Membr. Sci. 163 (2) (1999) 333–348.

[15] M. Khayet, Membranes and theoretical modeling of membrane distillation: A review, Adv. Colloid Interface Sci. 164 (1–2) (2011) 56–88.

[16] M.C. García-Payo, et al., Separation of binary mixtures by thermostatic sweeping gas membrane distillation: II. Experimental results with aqueous formic acid solutions, J. Membr. Sci. 198 (2) (2002) 197–210.

[17] S. Bandini, G.C. Sarti, Heat and mass transport resistances in vacuum membrane distillation per drop, AIChE Journal 45 (1999) 1422–1433.

[18] K.W. Lawson, D.R. Lloyd, Membrane distillation. I. Module design and performance evaluation using vacuum membrane distillation, J. Membr. Sci. 120 (1) (1996) 111–121.

[19] F. Laganà, G. Barbieri, E. Drioli, Direct contact membrane distillation: modeling and concentration experiments, J. Membr. Sci. 166 (1) (2000) 1–11.

[20] Y. Fujii, et al., Selectivity and characteristics of direct contact membrane distillation type experiment. I. Permeability and selectivity through dried hydrophobic fine porous membranes, J. Membr. Sci. 72 (1) (1992) 53–72.

[21] M. Gryta, Concentration of saline wastewater from the production of heparin, Desalination 129 (1) (2000) 35–44.

[22] M.D. Kennedy, et al., Water treatment by microfiltration and ultrafiltration, in: A. Li, et al., (Eds.), Advance Membrane Technology and Application, John Wiley, New Jersey, 2008.

[23] S. Cerneaux, et al., Comparison of various membrane distillation methods for desalination using hydrophobic ceramic membranes, J. Membr. Sci. 337 (1–2) (2009) 55–60.

[24] M. Khayet, A. Velázquez, J.I. Mengual, Direct contact membrane distillation of humic acid solutions, J. Membr. Sci. 240 (1–2) (2004) 123–128.

[25] S. Srisurichan, R. Jiraratananon, A.G. Fane, Humic acid fouling in the membrane distillation process, Desalination 174 (1) (2005) 63–72.

[26] P. Termpiyakul, R. Jiraratananon, S. Srisurichan, Heat and mass transfer characteristics of a direct contact membrane distillation process for desalination, Desalination 177 (1–3) (2005) 133–141.

[27] S. Gunko, et al., Concentration of apple juice using direct contact membrane distillation, Desalination 190 (1–3) (2006) 117–124.

[28] Z. Ding, R. Ma, A.G. Fane, A new model for mass transfer in direct contact membrane distillation, Desalination 151 (3) (2003) 217–227.

[29] R.W. Schofield, et al., Factors affectingflux in membrane distillation, Desalination 77 (1990) 279–294.

[30] A. El-Abbassi, et al., Concentration of olive mill wastewater by membrane distillation for polyphenols recovery, Desalination 245 (1–3) (2009) 670–674.

[31] Y. Yun, et al., Direct contact membrane distillation mechanism for high concentration NaCl solutions, Desalination 188 (1–3) (2006) 251–262.

[32] S. Srisurichan, R. Jiraratananon, A.G. Fane, Mass transfer mechanisms and transport resistances in direct contact membrane distillation process, J. Membr. Sci. 277 (1–2) (2006) 186–194.

[33] P.P. Zolotarev, et al., Treatment of waste water for removing heavy metals by membrane distillation, J. Hazard. Mater. 37 (1) (1994) 77–82.

[34] K. Sakai, et al., Effects of temperature and concentration polarization on water vapour permeability for blood in membrane distillation, Chem. Eng. J. 38 (3)(1988) B33–B39.

[35] Zhang, Y.J., & Wu, X.M., et al. (2001). Application and development of membrane distillation. Journal of Filtration & Separation, 11(2):16-21.

[36] M. Khayet, T. Matsuura, Pervaporation and vacuum membrane distillation processes: Modeling and experiments, Ind. Eng. Chem. Res. 50 (2004) 1697–1712